Polymer Journal (2012) 44, 83–94

www.nature.com/pj

ORIGINAL ARTICLE

Structure and dynamics of poly(vinyl alcohol) gels in mixtures of dimethyl sulfoxide and water

Toshiji Kanaya[1], Nobuaki Takahashi[2], Hiroki Takeshita[3], Masatoshi Ohkura[4], Koji Nishida[1] and Keisuke Kaji[1]

We reviewed our structure studies on poly(vinyl alcohol) (PVA) gels formed in the mixtures of dimethyl sulfoxide (DMSO) and water using various scattering methods, including wide-, small- and ultra-small-angle neutron scattering and light scattering. These studies revealed the hierarchic structure of PVA gels formed in DMSO/water (60/40 v/v) in a very wide spatial scale from 1 Å to several micrometers. The crosslinking points are crystallites with radii of ~70 Å, the distance between the neighboring crystallites is 180–200 Å, and the bicontinuous structure due to liquid–liquid phase separation is in μm scale. We also review our dynamic studies on three kinds of PVA gels at the nanometer scale using neutron spin echo techniques to separate the concentration fluctuations observed by small-angle neutron scattering into the static and dynamics contributions.
Polymer Journal (2012) **44,** 83–94; doi:10.1038/pj.2011.88; published online 19 October 2011

Keywords: dynamics; gel; light scattering; neutron spin echo; phase separation; poly(vinyl alcohol); small-angle neutron scattering

INTRODUCTION

Poly(vinyl alcohol) (PVA) is obtained by the saponification of poly (vinyl acetate) by the addition of alkali. It cannot, however, be prepared by the polymerization of vinyl alcohol because the corresponding monomer, vinyl alcohol, is unstable and cannot be isolated. This fact was first discovered by Herrmann and Haehnel.[1,2] PVA is one of the most interesting synthetic polymers because it is water soluble and biocompatible, and the applications of PVA span various fields, including industrial and biomedical materials. Therefore, many scientific and application studies have been performed since its invention.

Here, we briefly discuss the history of science and engineering of PVA fiber according to Sakurada's book.[2] Herrmann *et al.*[3] also produced PVA fiber; they reported that the fiber could be made from PVA by the well-known wet and dry spinning methods, and the water resistance of the fibers could be improved by physical and chemical aftertreatment to make them suitable for use as textile fiber. Hermann *et al.* focused mainly on the solubility of the fiber in water because they intended to use this thread for surgical purposes to replace catgut and silk. Hence, they improved the water solubility but were not interested in the water resistance of the fiber. Studies on the water-resistant PVA textile fiber started in 1938 in Japan. Sakurada *et al.*[5] at Kyoto University prepared water-insoluble PVA fiber by wet spinning an aqueous solution of PVA using a sodium sulfate solution as a coagulation bath with the subsequent formalization of the fiber.[4] Furthermore, they succeeded in improving the hot-water resistance of the fiber by heat treating the wet-spun fiber in hot air.[4,6] The pilot plant for developmental work on this fiber was erected in 1942 on the campus of Kyoto University through the support of a semigovernmental organization. Immediately after the end of the Second World War, Kurashiki Rayon Co. (renamed to Kuraray Co., Kurashiki, Okayama, Japan) reactivated its second pilot plant and proceeded with extensive development studies.

They succeeded in establishing an industrial process for PVA as well as for the fiber; they also established plants for the production of both PVA and its fiber. Commercial production started in 1950. Thus, PVA and its fiber had an important role in polymer science as well as in the polymer industry in Japan. Extensive studies to find new functions and higher performances for PVA still continue in Japan.

One of the characteristic features of PVA is its gelation in various solvents upon cooling.[7–13] Hydrogels of PVA can be obtained from the aqueous solutions and are often used for tissue engineering.[14,15] The properties of PVA gels are well known to depend on the solvents and preparation methods.[9,16] For example, PVA hydrogels prepared with free-thaw cycling show interesting features of transparency and a high modulus.[16] Hyon *et al.*[9] have reported PVA gels prepared in mixtures of DMSO and water, which also showed very interesting features that depend on the ratio of DMSO to water. When the ratio of DMSO to water is 0.8, the gel obtained at room temperature is transparent, whereas it is opaque for the ratio of 0.6. Furthermore, when the PVA in a mixture of DMSO and water at a ratio of 0.6 is quenched to temperatures less than ~−20 °C, the obtained gels are transparent. Thus, the properties of the gels in mixtures of DMSO and water are interesting, and the gels provide good examples for investigations of the gel structure and the gelation mechanism.

For the past two decades, we have studied the structures and structure formation processes of PVA gels on a wide scale using

[1]Institute for Chemical Research, Kyoto University, Uji, Japan; [2]Neutron Science Section, Materials and Life Science Division, J-PARC Center, Japan Atomic Energy Agency, Tokai, Japan; [3]Department of Materials Science and Technology, Nagaoka University of Technology, Nagaoka, Japan and [4]Films &Film Products Research Laboratories, Toray Industries, Inc., Otsu, Japan
Correspondence: Professor T Kanaya, Institute for Chemical Research, Kyoto University, Gokashi, Uji, Kyoto-fu 611-0011, Japan.
E-mail: kanaya@scl.kyoto-u.ac.jp
Received 25 April 2011; revised 21 July 2011; accepted 27 July 2011; published online 19 October 2011

techniques such as macroscopic observations,[12,13,17] wide-, small- and ultra-small-angle neutron scattering (WANS, SANS and USANS),[18–23] and light scattering.[24–27] In addition, neutron spin echo (NSE) measurements have also been performed to elucidate the dynamic properties of three kinds of PVA gels.[28–30] In this article, we review our previous results on the structure, structure formation process of PVA gels formed in mixtures of DMSO and water and the nanometer-scale dynamics for three kinds of PVA gels.

EXPERIMENTAL PROCEDURE

Materials and gel preparation

Fully saponified atactic PVA samples with a number-average degrees of polymerization P_n in the range of 186 to 20 200 were used. PVA with P_n=1700 was mainly used for the SANS, USANS and light scattering (LS) measurements. The molecular-weight distributions M_w/M_n are $\sim$2,[12] where M_w and M_n are the weight- and number-average molecular weights, respectively. The details of the characterization of the PVA samples have been reported previously.[12] Deuterated atactic PVA (PVA-d_4) was also employed for the WANS measurements. The number-average degree of polymerization P_n was 1700 and the M_w/M_n was 2.01. The solvent used for the WANS, SANS and USANS measurements was a mixture of deuterated DMSO (DMSO-d_6) and heavy water (D_2O). A mixture of protonated solvents was used for the macroscopic observations and the LS measurements.

Gel samples were prepared as follows. A given amount of PVA was dissolved in the solvent at $\sim$130°C to be homogenized in a sealed glass tube under vacuum to avoid contamination from atmospheric H_2O. After a second homogenization at 100 °C, the solution was quenched to various temperatures for gelation. The gelation time was macroscopically determined by a tilting method.

Measurements

WANS measurements were performed with a high-intensity total scattering spectrometer of time-of-flight (TOF) type installed at the pulsed thermal neutron source in the National Laboratory for High Energy Physics (KEK), Tsukuba, Japan. This spectrometer can cover a Q range from 0.5 to 50 Å^{-1} using neutron wavelengths of 0.3 to 4 Å.

SANS measurements were performed with the SAN spectrometer[31] at KEK, Tsukuba, Japan, the SANS-U spectrometer[32] at the JRR-3M reactor located at the Japan Atomic Energy Research Institute (JAERI), Tokai, Japan and the 30m-SANS spectrometer[33] at the High Flux Isotope Reactor located at Oak Ridge National Laboratory, Oak Ridge, TN, USA. The SAN spectrometer is a TOF-type small-angle scattering spectrometer installed at the pulsed cold neutron source. The Q ranges covered by the SAN, SANS-U and 30m-SANS spectrometers were 0.01 to 0.2 Å^{-1}, 0.003 to 0.1 Å^{-1} and 0.003 to 0.03 Å^{-1}, respectively. In all the SANS measurements, incoherent scattering contributions from hydrogen atoms of the gel samples were subtracted.

For USANS measurements, we used the ULS spectrometer[34] equipped with a Bonse–Hart camera installed at the cold neutron source in the JRR-3M reactor of JAERI. The wavelength of incident neutrons was 4.73 Å. The full width at half-maximum of the rocking curve was 4.4 s for the parallel setting of double crystals of Si 111 with five successive reflections. The Q range of 10^{-5} to 10^{-2} Å^{-1} was covered by the spectrometer. The observed scattering intensities were corrected for the smearing effect due to the line slit by assuming an infinite length of the silt.

Light-scattering measurements were performed with a Malvern Instruments System 4700 (Malvern Instruments, Ltd., Worcestershine WR14 1XZ, UK). using an Ar^+ laser (λ=488 nm, 75 mW) as a light source. The length of scattering vector $Q=4\pi n \sin Q/\lambda$,where n is the reflective index, was in the range of 3.6×10^{-4} to 3.4×10^{-3} Å^{-1}. To reduce the effects of inhomogeneity (speckle) of the samples, which arise from the gel structure itself, the measurements were performed by rotating the sample cell (10 mm ϕ).

RESULTS AND DISCUSSION

Sol–gel phase diagram of PVA solution in DMSO/water and transparency

Figure 1 shows the sol–gel phase diagram 24 h after quenching as a function of PVA concentration C_p and quenching temperature T_q for

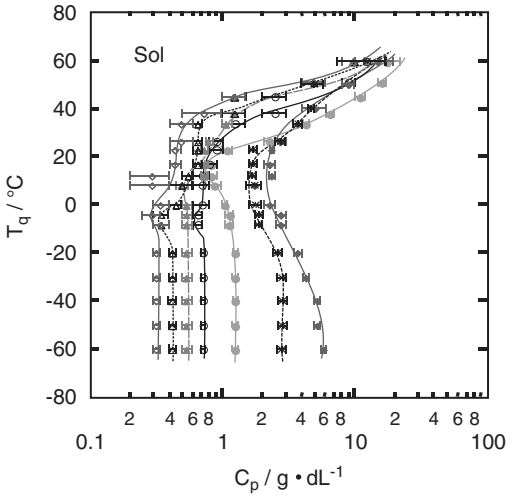

Figure 1 Sol–gel transition diagram of poly(vinyl alcohol) in a mixture of dimethyl sulfoxide and water (60/40 v/v). The degree of polymerization P_n=186 (♦), 590 (x), 1700 (●), 5430 (○), 10700 (▲), 11900 (Δ), 20200 (◇).

PVAs with various degrees of polymerization P_n in a mixture of DMSO and water (60/40 v/v).[12] The solid lines in the figure were drawn by eye. The time required for gelation (t_{gel}) depends on C_p, T_q and P_n. In general, t_{gel} increases as T_q increases and C_p and P_n decrease, which indicates that the sol–gel diagram depends on the standing time after quenching. We confirmed, however, that gelation was almost complete within 24 h for the examined ranges of T_q, C_p and P_n, although the gelation required more than 24 h at temperatures greater than 40 °C. Even in cases where the temperature exceeded 40 °C, the resulting phase diagram is similar to that obtained after a standing time of 24 h. The sol–gel transition curves in Figure 1 appear complicated, but the temperature dependence is almost identical for all the samples. Some distinct features depend on the range of T_q: (1) at temperatures less than ~-20 °C, the critical gelation concentration C^* was independent of T_q, except for the sample with the lowest degree of polymerization; (2) between ~-20 °C and $\sim+40$ °C, the lowest C^* was less than that observed at temperatures less than ~-20 °C; (3) at temperatures greater than $\sim+40$ °C, C^* increased rapidly with increasing T_q, and gelation was not observed at temperatures greater than $\sim+75$ °C.

We first consider the sol–gel transition curves at temperatures <-20 °C. In Figure 2, the average C^* for various T_q values at temperatures <-20 °C was plotted against P_n in double-logarithmic form. The slope of the straight line in the figure is -0.5, and the following relationship was obtained:

$$C^* = K(P_n)^{-0.5} \quad (1)$$

where K is a constant. This relationship implies that C^* is dominated by the chain overlap concentration of Gaussian chains. As shown in Figure 3, the gels formed at temperatures less than ~-20 °C were transparent, which suggests that gelation occurs homogeneously. Polymer chains should overlap when an infinite network is formed over the whole system in the homogeneous solution. A homogeneous solution with a concentration less than that of the overlap concentration cannot become a gel because crosslinking points do not connect over the system. Therefore, chain overlap in the homogeneous solution is necessary for gelation. The overlap concentration $C^*_{R_g}$ is given by

$$C^*_{R_g} = \frac{M_W}{(4/3)\pi\langle R_g^2\rangle^{3/2}} \quad (2)$$

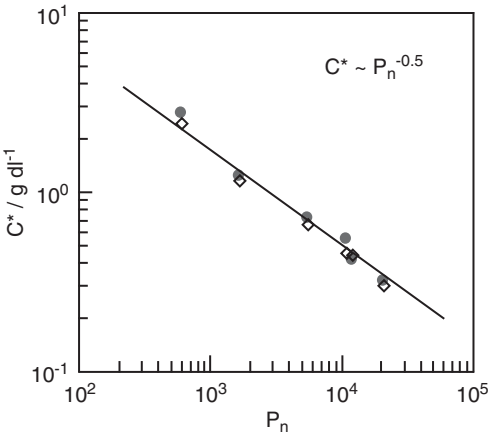

Figure 2 Critical gelation concentration C^* (●) and the calculated overlap concentration $C^*_{R_g}$ (◇) as a function of the degree of polymerization P_n in the temperature range of −20 to −60 °C.

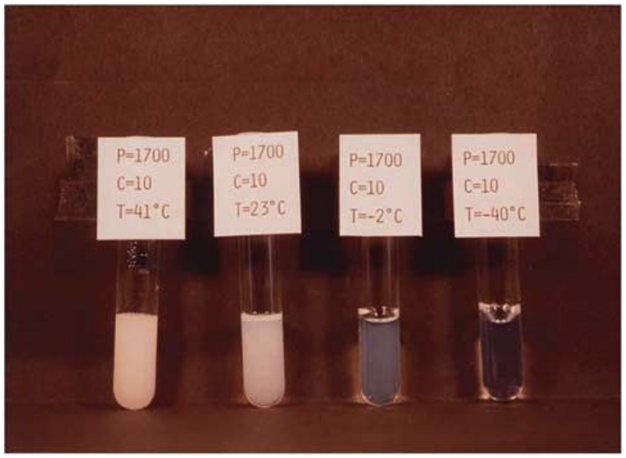

Figure 3 Photographs of poly(vinyl alcohol) gels in mixtures of dimethyl sulfoxide and water (60/40 v/v) at various gelation temperatures T_qs. T_q=41, 23, −2, −40 °C from left to right.

where M_w is the weight-average molecular weight and $\langle R_g^2 \rangle$ is the mean square radius of gyration of the polymer chain. The term $\langle R_g^2 \rangle$ is given by equation (3) under the Gaussian chain approximation with a molecular-weight distribution $U=M_w/M_w-1$:[35]

$$\langle R_g^2 \rangle = \frac{bL(2U-1)}{3(U+1)} \tag{3}$$

where b is the persistence length and L is the contour length. Equations (2) and (3) give the relationship:

$$C^*_{R_g} = \frac{m(U+1)}{\frac{4}{3}\pi[bl_0(2U+1)/3]^{3/2}} (P_n)^{-1/2} \tag{4}$$

where m and l_0 are the molecular weight and the length of the PVA monomer unit, respectively. We calculated $C^*_{R_g}$ as a function of P_n from equation (4) by assuming a persistence length b of 7 Å. The plot in Figure 2 shows a good agreement between the calculated $C^*_{R_g}$ and the observed C^*. The overlap concentration could be calculated from the intrinsic viscosity, but this parameter was difficult to measure for the PVA in a mixture of DMSO and water (60/40 v/v) because of its aggregated nature.[19]

In the temperature range between ~−20 and ~40 °C, each sample exhibits a C^* value less than $C^*_{R_g}$. If the solution is homogeneous, gel formation is difficult at a concentration less than $C^*_{R_g}$ because all the polymer chains cannot contact. These results therefore suggest that gelation in this temperature range occurs in the heterogeneous solution, similar to gelation in an aqueous solution of PVA.[8] The origin of the heterogeneity may be liquid–liquid phase separation or spinodal decomposition (SD). These possibilities are implied by the gels in this temperature range being translucent or opaque (see Figure 3). After the spinodal phase separation, the structures of the solutions consist of two phases: the polymer-rich and polymer-poor phases. The polymer-rich phase exhibits a network-like bicontinuous structure over the whole system. When the concentration of PVA in the polymer-rich phase is greater than $C^*_{R_g}$, gelation can occur. The whole system becomes a gel because of the connectivity of the polymer-rich phase, even though the macroscopic average concentration is less than the overlap concentration. Consequently, C^* is less than $C^*_{R_g}$ between ~−20 °C and ~+40 °C.

At temperatures greater than that corresponding to the lowest C^*, C^* increased with an increase in the quenching temperature T_q. This result may be explained by taking into account that the crosslinking points in the PVA gel are crystallites. With respect to crystallization, PVA is regarded as a copolymer of different stereoisomers, and only the syndiotactic-rich sequences are available for crystallization.[36,37] According to the theory of crystallization in copolymers proposed by Flory,[38] sequences longer than the minimum stable crystallite length at equilibrium, which increase with temperature, can convert to crystallites. The number of syndiotactic sequences longer than the minimum length per chain, or the number of crystallites, therefore decreases with increasing temperature. Consequently, C^* increases with temperature. The leveling off of the sol–gel curves was observed at 70–75 °C for all the PVA samples. The equilibrium dissolution temperature of the PVA crystals in the DMSO/water solution was greater than 75 °C.

As previously discussed, the macroscopic measurements such as sol–gel diagram and transparency provided substantial information about the PVA gels; however, the structure and the formation mechanism of the PVA gels at the molecular level must be clarified to allow control of the final structure. We therefore investigated the structure of PVA gels using WANS, SANS and USANS, as well as LS.

Structure and structure formation process of PVA gels in DMSO/water

Structure of crosslinking points. PVA is a typical crystalline polymer; crosslinking points in the gels are therefore believed to be crystallites, although this hypothesis has never been directly confirmed.[19] We conducted WANS measurements of deuterated PVA (PVA-d_4) gel at a PVA concentration of 10 g dl^{-1} in a mixture of DMSO-d_6 and D_2O (60/40 v/v) at 23 °C. The observed scattering intensity $I(Q)$ is shown for the gel in Figure 4a in the Q range of 0.8 to 10 Å^{-1}. Figure 4b was obtained when the scattering intensity of the solvent was subtracted from that of the gel after correcting for the volume of solvent molecules replaced by PVA molecules. The strongest peak was observed at Q=1.39 Å^{-1}, which corresponds to the Bragg diffractions from the (101) and (10$\bar{1}$) planes of the PVA crystals. For comparison, the scattering curve from a PVA-d_4 solid film measured on the neutron diffractometer is also shown in Figure 4c. The difference between the scattering curves of the gel and the solvent (Figure 4b) is similar to that of the solid film, although the widths of the peaks in the difference scattering curve are broader than those of the film. This difference may be due to the small crystallites in the gel. The existence

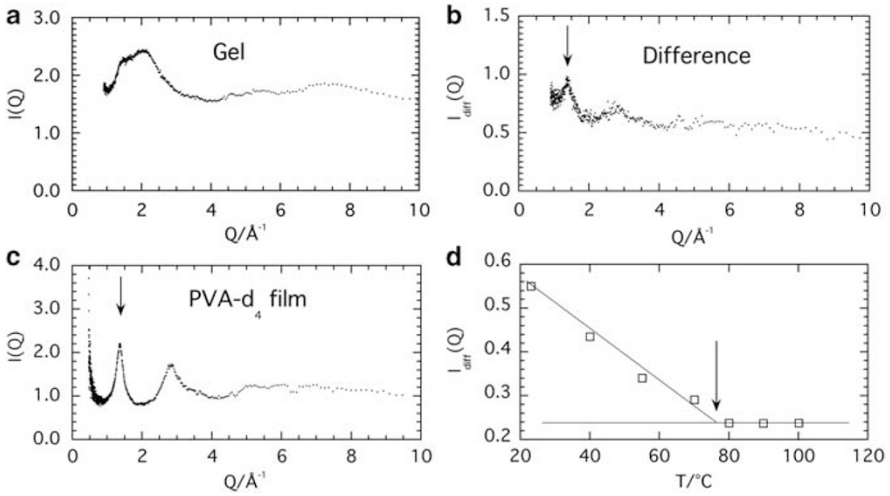

Figure 4 Wide-angle neutron scattering intensity $I(Q)$. (**a**) Poly(vinyl alcohol) (PVA)-d_4 gel in dimethyl sulfoxide (DMSO)-d_6/D_2O (60/40 v/v) with C_p=10 g dl^{-1}. (**b**) Difference intensity between the PVA-d_4 gel and the solvent. The subtraction was made by taking into account the solvent molecules replaced by PVA-d_4 in the gel. (**c**) PVA-d_4 solid film. The degree of crystallinity is ~45%. (**d**) Temperature dependence of the scattering intensity at the Bragg position (Q=1.39 Å^{-1}).

of crystallites in the PVA gel was confirmed, although at this stage whether they were the crosslinking points in the PVA gel had not been determined.

To confirm that the crystallites were the crosslinking points, WANS measurements were conducted as a function of temperature. The measurements were focused on the strongest Bragg peaks at Q=1.39 Å^{-1}. The intensity at Q=1.39 Å^{-1} gradually decreased with increasing temperature, and the Bragg peaks were no longer observed in the scattering curve at temperatures greater than 75 °C. This temperature agreed well with the melting temperature of the PVA gels determined by macroscopic observation,[12] which confirms that the crosslinking points of the PVA gel are crystallites. This fact gives us a basis for interpreting the SANS data presented in the next section.

Size and distribution of crosslinking points. SANS measurements were performed on the PVA gels in DMSO-d_6/D_2O (60/40 v/v) at 23 °C in a Q range from 0.01 to 0.1 Å^{-1} using a small-angle scattering machine at KEK.[19] Figures 5a shows the scattering intensities $I(Q)$s of the PVA gels with C_p=2, 5 and 10 g dl^{-1}, which were plotted in double-logarithmic form after being normalized against C_p. In the Q range above ~0.05 Å^{-1}, the scattering intensity $I(Q)$ decreased with increasing Q according to the 4th power law for all the concentrations:

$$I(Q) \sim Q^{-4} \tag{5}$$

This Q dependence corresponds to the so-called Porod's law, which indicates that the surfaces of the crystallites in the PVA gels are very smooth.[39] Figure 5b shows the inverse of the scattering intensity $I(Q)^{-1}$ plotted against Q^2 in the Q range below 0.045 Å^{-1}. A linear relationship was obtained for all the concentrations, which means that the Q dependence of $I(Q)$ in the Q range below ~0.035 Å^{-1} can be described by the Ornstein–Zernike formula

$$I(Q) = \frac{I(0)}{(1+\xi^2 Q^2)} \tag{6}$$

where ξ is a correlation length and $I(0)$ is the scattering intensity at Q=0. The concentration dependence of the correlation length ξ is shown in Figure 6a. The values of ξ in the gel were ~180 Å and were almost independent of the concentration C_p. Because the crosslinking points of the PVA gels are crystallites, the correlation length ξ is governed by the inter-crystallite correlations because the correlations between the crystallites are very strong compared with other correlations, such as those between non-crystallized polymer chain segments. If the crosslinking points were homogeneously distributed in the whole system, the correlation length, which is regarded as an average nearest-neighbor crystallite distance, would decrease with an increase in the polymer concentration according to $C_p^{-1/3}$. However, this was not the case. As previously discussed, liquid–liquid phase separation occurred in the PVA solution at 23°C, and the solution was separated into polymer-rich and polymer-poor phases before gelation. According to the theory of phase separation,[40] the polymer concentrations of polymer-rich and polymer-poor phases are thermodynamically determined to be independent of the total polymer concentration. Consequently, the structure within the polymer-rich phase should be independent of the total polymer concentration, as schematically illustrated in Figure 6b. Because the crystallites are mainly produced in the polymer-rich phase and because the scattering intensity is governed by the strongest correlation between the nearest-neighbor crystallites, the correlation length is almost independent of the PVA concentration.

To observe other aspects of the scattering curve, we calculated the distance distribution function $P(r)$, which is defined by the inverse Fourier transformation of the scattering intensity $I(Q)$,[41]

$$\begin{aligned} P(r) &\sim (2/\pi) rQI(Q)\sin(rQ)\mathrm{d}Q \\ &\sim 4\pi r^2 g(r) \end{aligned} \tag{7}$$

where $g(r)$ is a pair correlation function. The calculated distance distribution function $P(r)$ is shown in Figure 7 for C_p=5 g dl^{-1}. Two broad peaks or shoulders were observed at ~70 and 180~200 Å in $P(r)$ for all the PVA concentrations. Based on the previous discussion on the small-angle scattering intensity $I(Q)$, the peaks or shoulders at ~70 Å and 180~200 Å were assigned to the intra- and inter-crystallite correlations, respectively. To separate the two contributions, we fitted the observed $P_{intra}(r)$ in the small r range with a model function under the assumption that the shape of the crystallite was spherical and that the size distribution of crystallites in a given radius could be represented by a Gaussian function. The results of the fit are

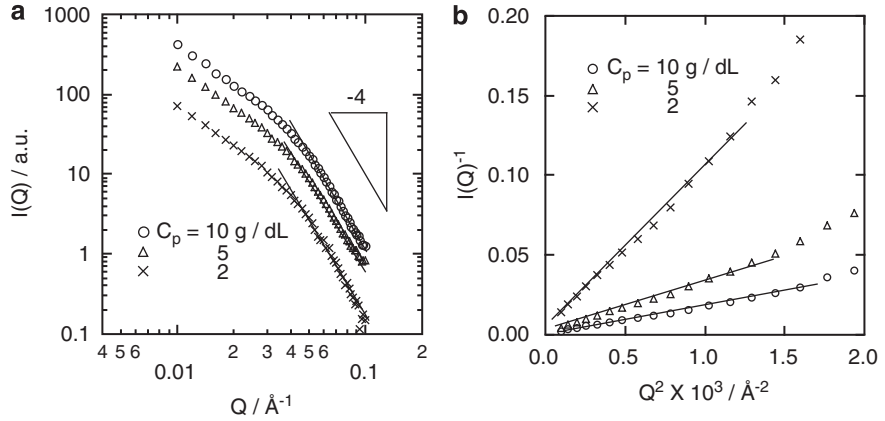

Figure 5 Small-angle neutron scattering intensity $I(Q)$ of poly(vinyl alcohol) gel in dimethyl sulfoxide /water (60/40 v/v) for C_p=2, 5, 10 g dl^{-1}. (**a**) Double logarithmic form, (**b**) $I(Q)^{-1}$ vs Q^2.

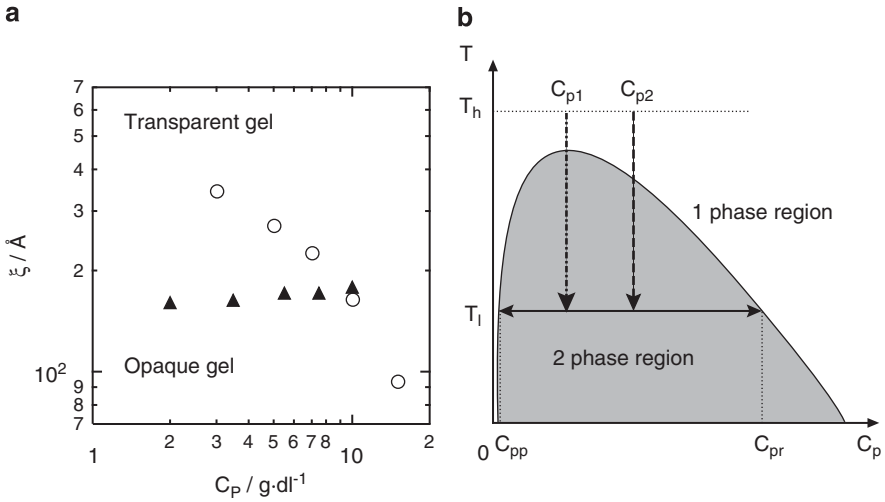

Figure 6 (**a**) Correlation length ξ of the opaque poly(vinyl alcohol) (PVA) gels (▲) and the transparent PVA gel (○) as a function of PVA concentration C_p. (**b**) Schematic sketch of the phase-separation curve.

shown in Figure 7 by dotted and dashed lines, which correspond to the intra-crystallite correlation $P_{intra}(r)$ and the inter-crystallite correlation $P_{inter}(r)$, respectively. The radii of the crystallites were ~73 Å, and the size distributions or the roots of the dispersion were ~15 Å for all the PVA concentrations.

We extended the Q range in SANS measurements down to 0.003 Å^{-1} to observe structural differences between the opaque and transparent gels.[20,22] The former gel was the same sample as that discussed in the previous section. The latter gel was prepared using two methods: by quenching a homogeneous DMSO-d_6/D_2O (60/40 v/v) solution of PVA to −40 °C, and from the mixture of DMSO-d_6/D_2O (80/20 v/v) at 23 °C. In Figures 8a and b, the scattering intensities $I(Q)$s of the opaque and transparent gels with C_p=0.5, 2, 5, and 10 g dl^{-1} are plotted. Interestingly, the $I(Q)$ of the transparent gels obeys the Ornstein–Zernike formula in the low Q range down to 0.003 Å^{-1}, whereas the $I(Q)$ of the opaque gel shows an upturn below ~0.008 Å^{-1}. These results indicate that the opaque gels exhibit a larger structure or heterogeneity than the network structure. This heterogeneity was expected to arise from the structure because of the phase separation, as previously discussed. Transparent gels formed in a mixture of DMSO-d_6/D_2O (80/20 v/v) at 23 °C did not exhibit such an upturn in $I(Q)$.

The correlation length ξ was evaluated for the transparent gels using the Ornstein–Zernike formula and plotted as a function of C_p in Figure 6. The correlation length ξ of the transparent gels decreases with an increase in the PVA concentration C_p according to a power law of $\xi \sim C_p^{-1/3}$, except for C_p=15 g dl^{-1}, which suggests that the crosslinking points (crystallites) are fairly homogeneously distributed in the gels. This homogeneous distribution is consistent with the idea that the phase separation does not occur in the transparent gels.

Phase separation before gelation for opaque gels. To obtain direct evidence for the phase separation, time-resolved LS measurements on DMSO/H_2O (60/40 v/v) solutions of PVA were performed after the solutions were quenched to 23 °C from 100 °C.[25] Figure 9 shows the observed time evolution of $I(Q)$ for a PVA solution with C_p=5 g dl^{-1} up to 237 min after the sample was quenched. The gelation time t_{gel} for the PVA solution at 23 °C was macroscopically determined to be ~180 min. The scattering intensity $I(Q)$ exhibits a maximum at ~Q=1.1×10^{-3} Å^{-1}, and the maximum position Q_m did not change

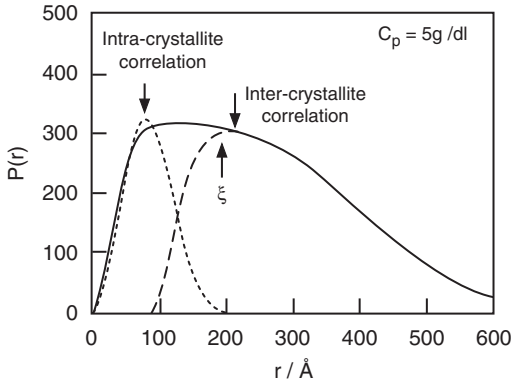

Figure 7 Distance distribution function $P(r)$ of poly(vinyl alcohol) gel in dimethyl sulfoxide /water (60/40 v/v) for C_p=5 g dl^{-1}. Dotted and dashed lines correspond to the distance distribution functions due to the intracrystallite correlation $P_{intra}(r)$ and intercrystallite correlation $P_{inter}(r)$, respectively.

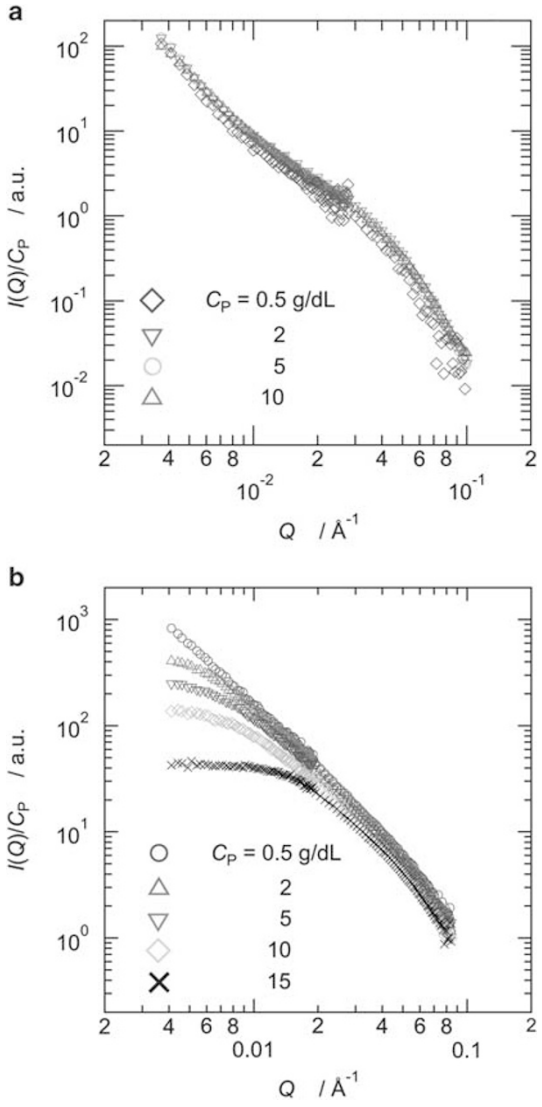

Figure 8 Small-angle scattering intensity of (**a**) the opaque gels in dimethyl sulfoxide (DMSO)/water (60/40 v/v) and (**b**) the transparent gels in DMSO/water (80/20 v/v). A full color version of this figure is available at *Polymer Journal* online.

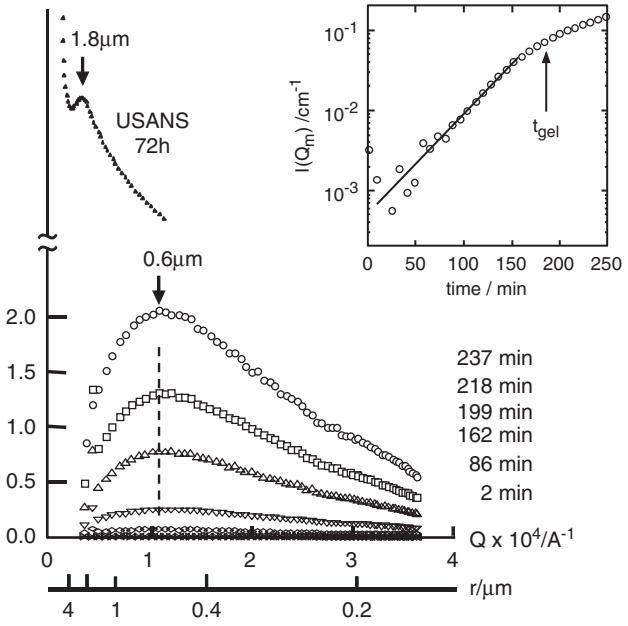

Figure 9 Time evolution of light-scattering intensity of a poly(vinyl alcohol) solution in dimethyl sulfoxide/water (60/40 v/v) just after being quenched to 25 °C from 100 °C, and ultra-small-angle neutron scattering (USANS) intensity 3 days after being quenched. The inset shows the time evolution of the light-scattering intensity at the peak position in semi-logarithmic form.

during the measurements. However, the intensity I_m at the maximum position Q_m increased according to an exponential law in the early stage, before ca. 170 min (see inset of Figure 9). These facts agree with the predictions for the early stage of SD,[42,43] which again confirms that the phase separation or SD occurred in the DMSO/H_2O (60/40 v/v) solution of PVA during the gelation process. The characteristic length in the early stage of the phase separation was calculated to be 0.57 μm through the relation $2\pi/Q_{max}$. The evolution rate of the maximum intensity slowed as the process approached the gelation time t_{gel} (=180 min), which suggests that the structural growth due to the phase separation is hindered by the elasticity of the network.

As previously discussed, the LS technique is a powerful tool for observing the phase-separation process at the micrometerscale. However, LS measurements were limited to fairly transparent samples. In the late stages of the phase separation, the PVA gels are so opaque that LS measurements are impossible. We therefore employed a USANS technique to see the structure in this case. Figure 9 shows the observed SANS intensity $I(Q)$ for an opaque PVA gel 3 days after being quenched to 23 °C,[21] the starting sample of which was the same as that used for the LS measurements. A broad maximum was observed in $I(Q)$ at Q=0.35×10^{-3} Å^{-1}, giving the characteristic lengths of 1.8 μm. This result suggests that the structural growth in the late stages of the phase separation proceeds against the elasticity of the gel network.

Phase separation after gelation for the transparent gel. We also investigated the structural evolution of a homogeneous transparent PVA gel that was prepared by quenching a homogeneous PVA solution in DMSO/water (60/40) from 100 °C to −40 °C.[26] Although the gel was essentially in the unstable two-phase region at −40 °C, the phase separation barely proceeded within the usual laboratory time because the earlier produced network resisted phase separation and the

molecular mobility was very low at this temperature. Consequently, we observed the time dependence of the volume and transparency of the gel after the temperature was increased to 25 °C. In addition, time-resolved LS measurements were performed to observe the microscopic structural formation.

We measured the volume change as a function of time immediately after the temperature increased to 25 °C. The observed ratio of the volume V to the initial volume V_0 is shown in Figure 10a. No appreciable change of the volume was observed in the initial 2 min, but then the volume began to gradually decrease (syneresis) and leveled off after ~500 min. This result indicates that the gel may have been in a state of apparent volume equilibrium after ~500 min. We measured the UV transmittance of the gel under the same experimental conditions to observe the transparency as a function of time after the temperature increase to 25 °C. The change of the transmittance is shown in Figure 10b; the data were corrected for the effects of volume change. The transmittance began to decrease immediately after the temperature increase and became 87% of the initial transmittance after 2 min. This result suggests that the SD-type phase separation of the gel proceeds at 25 °C. To confirm this phase separation, we performed time-resolved LS measurements after a temperature increase from –40 °C to 25 °C. The time evolution of the observed scattering intensities $I(Q)$ is shown in Figures 11a and b. The scattering intensity $I(Q)$ at t=0 min observed at –20 °C was almost independent of Q and exhibited no special structure in the observed Q range. However, the intensity $I(Q)$ after 2.5 min exhibits a broad peak at $\sim 1.6\times10^{-3}$ Å^{-1}, which corresponds to a characteristic wavelength Λ_m=0.39 μm, and $I(Q)$ increased exponentially with time without a change in the peak position. These are the characteristic features of the early stages of SD-type phase separation. As evident in Figure 11b, the intensity curve $I(Q)$ slightly increased from 34 min to 1080 min; both the peak intensity and the position Q_m remained almost constant, which suggests a phase separation of the gel network where the domain growth was extremely suppressed due to the elasticity of the network. After 1080 min, however, the decrease of the intensity near the peak position was clearly discernible. Such a decrease must correspond to the relaxation process during the transition to a new equilibrium state of two macroscopic phases that consist of an almost pure solvent phase and a shrunk swollen network phase.

Hierarchic structure of opaque gel. As previously discussed, we investigated the structure of opaque PVA gels in DMSO/water (60/40 v/v) in a wide spatial scale from 1 Å to several micrometers using various scattering methods.[24] In the nanometer region, we observed by WANS measurements that the crosslinking points are crystallites; the SANS measurements revealed that the radius of the crystallites is ~70 Å and that the distance between nearest crystallites is 180–200 Å. In addition, we determined that the surface of the crystallites is smooth according to Porod's law. The LS studies showed that the

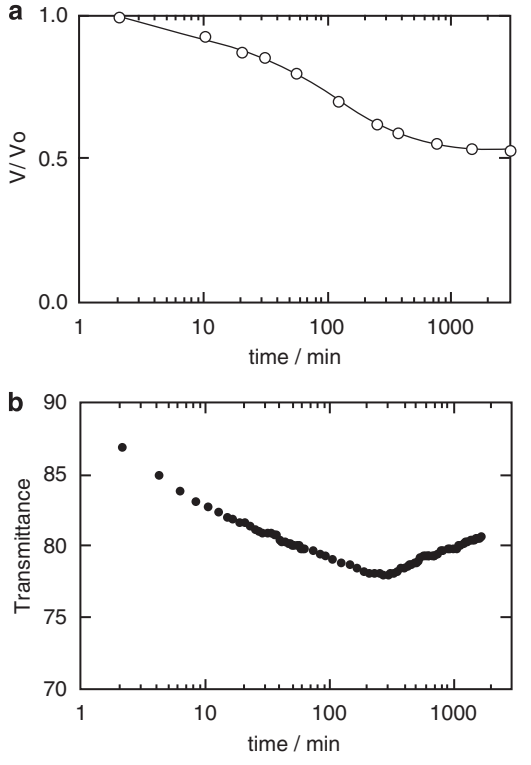

Figure 10 (**a**) Change in the volume and (**b**) change in the ultraviolet transmittance for poly(vinyl alcohol) gel formed in a mixture of dimethyl sulfoxide/water (60/40 v/v) at −40 °C after a temperature increase to 25 °C.

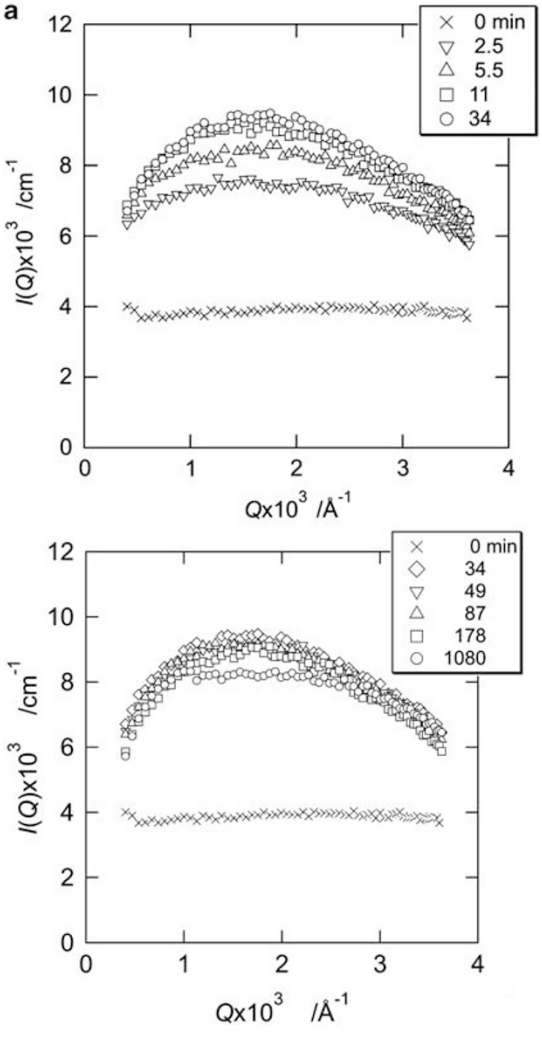

Figure 11 Time evolution of light-scattering intensity $I(Q)$ of poly(vinyl alcohol) gel formed in a mixture of dimethyl sulfoxide/water (60/40 v/v) at −40 °C after a temperature increase to 25 °C. (**a**) From 0 to 34 min and (**b**) from 34 to 1080 min after the temperature jump. A full color version of this figure is available at *Polymer Journal* online.

SD-type liquid–liquid phase separation occurs before gelation, which produces the polymer-rich and polymer-poor phases. The polymer-rich phase exhibits a bicontinuous structure, and crystallization mainly occurs in this phase, which results in an opaque gel due to network structure of the bicontinuous phase. The hierarchic structure of the opaque PVA gel revealed here is schematically described in Figure 12 with the scattering curves in a wide Q range from 10^{-4} to $10\,\text{Å}^{-1}$.

Gel formation mechanism. Based on the above observations, we propose the formation mechanism of the PVA gels in DMSO/water (60/40 v/v), which is schematically represented in Figure 13. At temperatures greater than $\sim -20\,^{\circ}\text{C}$, the rate of the phase separation is faster than the crystallization rate or the formation rate of crosslinking points. Therefore, the SD-type phase separation occurs in the solution to separate the polymer-rich and polymer-poor phases before gelation. The formation of crosslinking points occurs in the polymer-rich phase of the bicontinuous structure, which results in the opaque gels. In contrast, at temperatures less than $\sim -20\,^{\circ}\text{C}$, the crystallization rate is faster than the rate of the phase separation. Consequently, the gelation occurs in a homogeneous solution, which results in a transparent gel. However, the gel is not in the stable state, but rather in the unstable two-phase region. Then, the phase separation occurs very slowly in the gel against the elasticity of the gel network to finally enter into a new stable state of the macroscopic two phases of almost-pure solvent and a shrunk swollen gel.

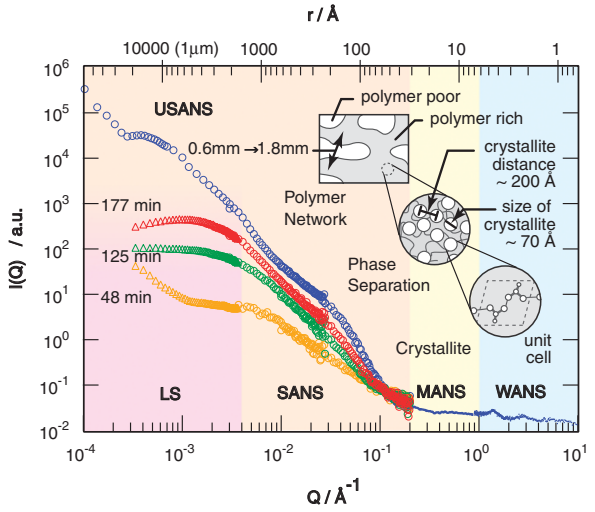

Figure 12 Scattering curves of poly(vinyl alcohol) gel formed in a mixture of dimethyl sulfoxide/water (60/40 v/v) at 25 °C in a wide Q range from 10^{-4} to $10\,\text{Å}^{-1}$, which corresponds to a real space from several micrometers to ~1Å. A schematic sketch of hierarchic structure of the gel in a real space is also shown in the inset.

Dynamics in the nanometer scale for three kinds of PVA gels

As detailed in the previous section, we investigated the structure and the structure formation processes of the PVA gels in DMSO/water (60/40 v/v). Studies of the gel dynamics are necessary to understand the response of the PVA gels to external fields such as temperature, pH and electric fields. For this purpose, we investigated the dynamics of three types of PVA gels in a spatial scale of nanometers to several tens of nanometers using a NSE technique.[44] The first PVA gel was a physical gel formed in DMSO/water (60/40 v/v), the structure of which was studied in the previous section. As previously discussed, the crosslinking point in the gel is a micro-crystallite, and hence the lifetime is infinite unless the gel is heated to temperatures greater than the dissolution temperature of the crystallite. The second gel was a PVA gel in aqueous borax solution. The complex formation between hydroxy groups of PVA and a borate anion acts as a crosslinking network, the lifetime of which is finite because of the exchange of hydrogen bonding. The third gel was a PVA gel chemically crosslinked by glutaraldehyde (GA). In this case, the lifetime of the crosslinking points becomes infinite because of their permanent chemical bonds. We have performed NSE measurements on these three PVA gels to compare their characteristic dynamic features.

PVA gels in DMSO/water. As discussed in the previous section, the crosslinking points of the network are crystallites. The distance

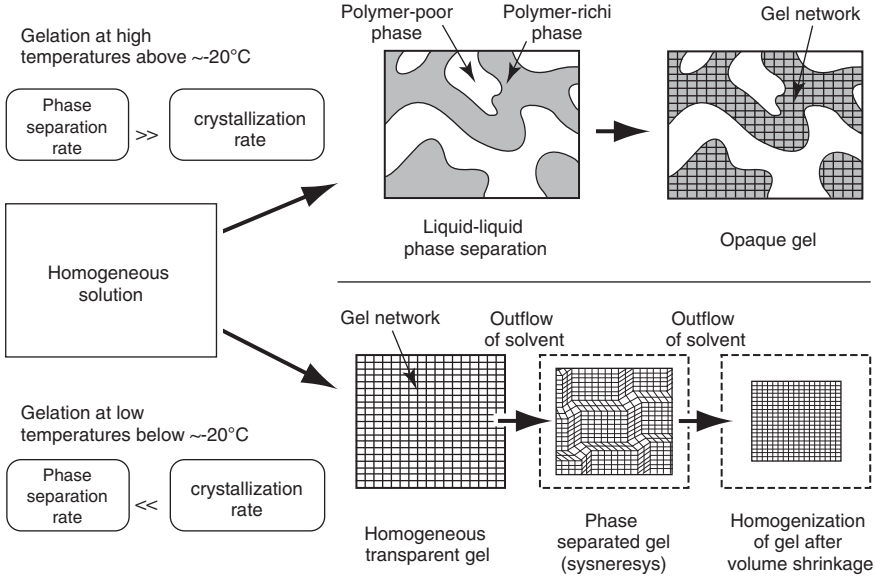

Figure 13 Formation mechanism of poly(vinyl alcohol) gels in dimethyl sulfoxide/water (60/40 v/v) at temperatures greater than and less than $\sim -20\,^{\circ}\text{C}$, which gives opaque and transparent gels, respectively.

between the nearest neighboring crystallites is ~180–200 Å, and the crystallites' radii are ~70 Å. In the Q-range between 0.02 and 0.1 Å^{-1}, Porod's law [$I(Q) \sim Q^{-4}$] was observed for the SANS measurements, which was attributed to the smooth surfaces of the crystallites. This Q range almost corresponds to the Q range in the present NSE measurements, which implies that we mainly observed the dynamics of the crosslinking points or the crystallites in the PVA gel.[28,29]

Fluctuations of the scattering length density or the concentration in the PVA gel can be observed in the SANS measurements. It is estimated using[45]

$$I(\boldsymbol{Q}, t=0) = N^{-1} \sum_{i=1}^{N} \sum_{j=1}^{N} \langle \exp[-i\boldsymbol{r}_i(0)\boldsymbol{Q}] \exp[i\boldsymbol{r}_j(0)\boldsymbol{Q}] \rangle \quad (8)$$

where N is the number of scattering elements, $\mathbf{r}_i(0)$ and $\mathbf{r}_j(0)$ are the positions of the i-th and j-th elements, respectively, and $\langle \ldots \rangle$ means the ensemble average. This estimation corresponds to a time correlation function of $\exp[-i\boldsymbol{r}(t)\boldsymbol{Q}]$ at t=0. In the NSE measurements, however, the time evolution of fluctuations or the so-called coherent intermediate scattering function $I(Q,t)$, can be observed and is given by[45]

$$I(\boldsymbol{Q}, t) = N^{-1} \sum_{i=1}^{N} \sum_{j=1}^{N} \langle \exp[-i\boldsymbol{r}_i(0)\boldsymbol{Q}] \exp[i\boldsymbol{r}_j(t)\boldsymbol{Q}] \rangle \quad (9)$$

If the fluctuations are time dependent, $I(Q,t)$ decays with time. If they are frozen, however, $I(Q,t)$ is independent of time and remains constant. The former and the latter cases are called static (or frozen) and dynamic fluctuations, respectively. We cannot distinguish the dynamic and static fluctuations in the SANS measurements.

To observe the time-dependent and/or time-independent fluctuations, we evaluated the normalized intermediate scattering function $I(Q,t)/I(Q,0)$ using the NSE. The observed $I(Q,t)/I(Q,0)$ is shown in Figure 14 at Q=0.04, 0.07, 0.10 and 0.12 Å^{-1}. In a short time region below about 3 ns, $I(Q,t)/I(Q,0)$ decayed rapidly, whereas it did not decay and remained constant in the longer time range. The observed intermediate scattering function can be phenomenologically described by $I(Q,t)/I(Q,0)=f_n(Q)+[1-f_n(Q)]F(Q,t)$, where $f_n(Q)$ is a fraction of the non-decaying component and $F(Q,t)$ is a generalized decay function. Assuming that the decay function could be expressed by a single exponential function, we fitted the equation to the observed intermediate functions to evaluate the relaxation time τ_f and the fraction of the non-decaying component $f_n(Q)$ as a function of Q. The results of the fits are shown by solid curves in Figure 14, which shows good agreement with experimental curves within the experimental accuracy. The fractions of the non-decaying component $f_n(Q)$ and the rest $[1-f_n(Q)]$ correspond to those of the static and dynamic fluctuations, respectively. The observed total SANS intensity $I(Q)$ was then divided into the static $f_n(Q)I(Q)$ and dynamic fluctuations $[1-f_n(Q)]I(Q)$. The results are shown in Figure 15. The total SANS intensity was primarily governed by the static fluctuations in the PVA gel, which indicates that the molecular motions in the PVA gel were almost frozen, at least in that Q range.

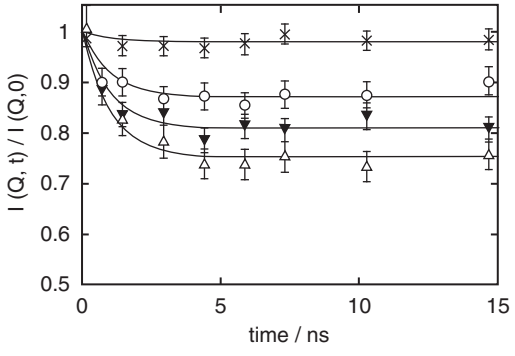

Figure 14 Normalized intermediate scattering function $I(Q,t)/I(Q,0)$ of poly(vinyl alcohol) gel in a mixture of dimethyl sulfoxide/water (60/40 v/v). Solid curves are the results of fits.

PVA gels in aqueous borax solution. We also studied the dynamics of PVA in an aqueous borax solution.[29] The viscosity of the aqueous solution with the PVA concentration C_p=2.4 wt% was about 2×10^{-3} Pa s^{-1}. The viscosity began to abruptly increase with the polymer concentration at $\sim C_p$=3.0 wt%; the viscosity is $\sim 4\times10^2$ Pa s^{-1} at C_p=4.8 wt%, which is more than five orders of magnitude greater than that of C_p=2.4%.[46,47] We designated the aqueous borax solutions of PVA with concentrations less than and greater than 3.0 wt% as PVA–borax sol and PVA–borax gel, respectively. In the aqueous borax solutions of PVA, the gelation process occurs through intermolecular hydrogen bonds between hydroxyl groups on PVA chains because of the intervention of a borate anion. The crosslinking points are therefore exchangeable, which results in the gel flowing extremely slowly.

Normalized intermediate scattering functions $I(Q,t)/I(Q,0)$ were measured by the NSE spectrometer for the PVA–borax sol with C_p=2.4 wt% and the PVA–borax gel with C_p=4.8 wt%. In contrast to $I(Q,t)/I(Q,0)$ of the PVA gel formed in a mixture of DMSO and water (60/40 v/v), the $I(Q,t)/I(Q,0)$ of these two solutions appeared to decay to zero at infinite time, even for the gel. The PVA–borax sol was a solution, and the Zimm model[48] or a bead-spring model with hydrodynamic interactions is known to describe well the polymer motions in solutions.[49] Therefore, we employed the Zimm model to analyze these intermediate scattering functions. The coherent intermediate scattering function was scaled using the so-called Zimm time $(Q^3t)^{2/3}$, as shown by de Gennes *et al.*[50] Therefore, the observed intermediate scattering functions were plotted against $(Q^3t)^{2/3}$ for the

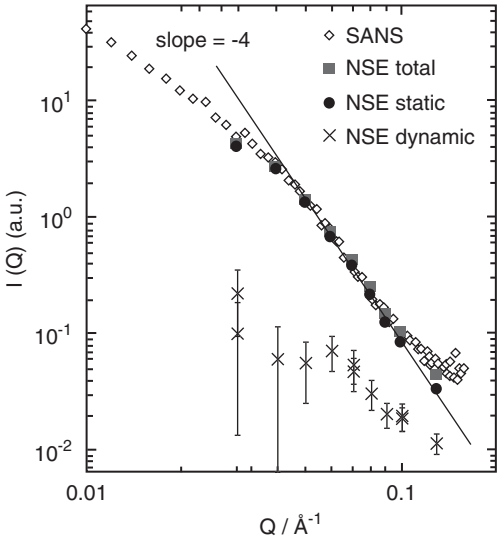

Figure 15 Small-angle neutron scattering intensity of poly(vinyl alcohol) gel in a mixture of dimethyl sulfoxide and water (60/40 v/v). (Δ): measured by small-angle neutron scattering (SANS) machine, (□): measured by neutron spin echo (NSE) spectrometer, (●): static (frozen) and (x): dynamic component in NSE total scattering intensity.

PVA–borax sol and the gel in Figures 16a and b, respectively. The data points fall on the theoretically calculated master curve, which suggests that the Zimm scaling works well for the sol and even for the gel. The ratio of the Zimm decay rate Γ_z of the gel to that of the sol is only 2.2, although the viscosity of the gel is more than five orders of magnitude greater than that of the sol. Surprisingly, the PVA–borax gel appeared as the sol with respect to the intermediate scattering function, at least in the Q range of 0.02 to 0.13 Å^{-1}. Why can the Zimm model describe the dynamics of the gel although it was developed for solution dynamics? To consider this problem, we examined the Q dependence of the first cumulant or the initial decay rate of $\ln[I(Q,t)/I(Q,0)]$ $(=\Gamma_i=-\mathrm{d}\{\ln[I(Q,t)/I(Q,0)]\}/\mathrm{d}t)$.

In Figure 17, the initial decay rate Γ_i is plotted vs Q for the PVA–borax sol and gel in a double logarithmic form. In the Q range above a certain critical value Q_c that is indicated by arrows in the figure, the Γ_i is proportional to Q^3 for both the sol and gel. This proportionality agrees with the Q dependence of the Zimm decay rate Γ_z,[50] which confirms again that the Zimm model is appropriate to describe the dynamics of both the sol and gel, at least above Q_c. However, the initial decay Γ_i is proportional to Q^2 in the Q range below the critical value Q_c, which must be the so-called gel mode.[51] This result suggests that the Zimm model is not appropriate in the low Q range below Q_c. The gel mode is a propagating mode on an elastic gel network, which permits propagation over a range larger than the mesh size of the network. The mesh size was approximately evaluated from the critical Q_c at the crossover between the Zimm and gel modes. The critical values Q_c were 0.060 and 0.075 Å^{-1} for the borax sol and gel, respectively, which resulted in mesh sizes $(2\pi/Qc)$ of 105 and 83.8 Å, respectively. The ratio of the Q_c of the sol to that of gel is 1.25, which is very close to $(2)^{1/3}$. This result means that the mesh size of the gel network is proportional to the –1/3 power of the PVA concentration, which suggests that the network structures of the sol and gel are rather homogeneous. The fact that the gel mode was observed in both the PVA–borax gel and sol may suggest that the gel mode originated from a temporal network owing to chain entanglements. Finally, we briefly consider the reason why the polymer chain motion in the gel, which was similar to that in the sol, is described by the Zimm model. If all borax molecules work as crosslinking points, one crosslinking point exists per 8.6 PVA monomers, on average. In this situation, polymer chains must undergo some constraint by the crosslinking points. However, the NSE measurements show that the polymer chains behave as if they have no crosslinking points on the spatial scale of several nanometers. This result strongly suggests that not all borax molecules participate in hydrogen bonding.

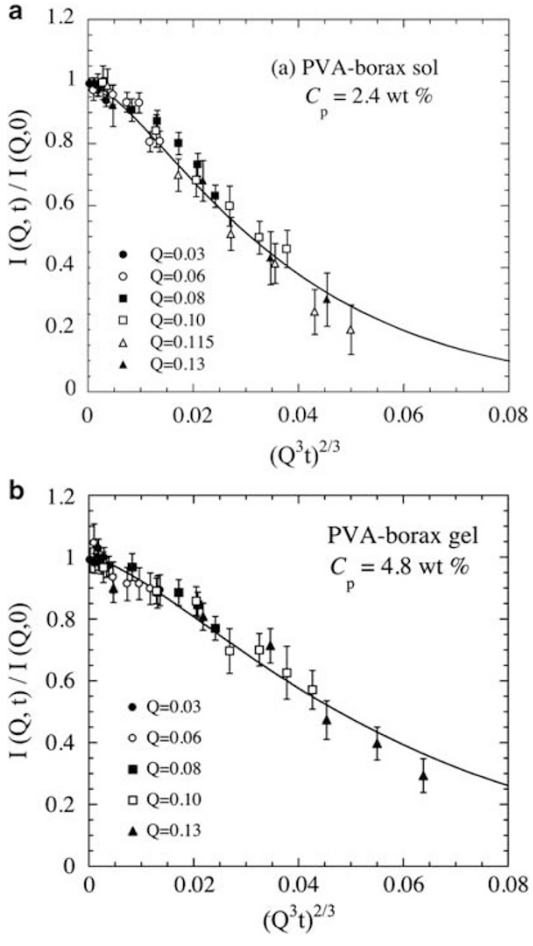

Figure 16 Zimm scaling of normalized intermediate scattering functions $I(Q,t)/I(Q,0)$ of (**a**) poly(vinyl alcohol)–borax sol with C_p=2.4 (wt% and (**b**) gel with C_p=4.8 wt%. (●): Q=0.03 Å^{-1}, (○): 0.06 Å^{-1}, (■): 0.08 Å^{-1}, (□): 0.10 Å^{-1}, (▲): 0.13 Å^{-1}. Solid curves are the Zimm master curves.

Chemically crosslinked PVA gels. SANS measurements were performed on the chemically crosslinked PVA gels with various concentrations of PVA C_p and GA C_g.[30] In Figure 18, the SANS intensities are shown for C_p=0.8 and 8 g dl^{-1} for various C_g values. In the case of C_p=0.8 g dl^{-1}, the SANS intensity increased in the low Q range below ~0.05 Å^{-1} as the GA concentration C_g increased, which suggests that the inhomogeneity in the gel increased with the crosslinking density. In contrast, the SANS intensity of the PVA gel with C_p=8 g dl^{-1} was independent of the GA concentration C_g. In the semi-dilute solutions of polymers (C_p=8 g dl^{-1}), the crosslinking between the polymer chains did not change the structure because the chains overlapped each other before crosslinking. This lack of structural change means that the structure of the semi-dilute polymer solution was similar to that of the gel in the static SANS measurements. However, the dynamic properties of the gel are expected to be different from the solution because of the crosslinking.

Normalized intermediate scattering functions $I(Q,t)/I(Q,0)$ of the gels were measured using the NSE spectrometer as a function of the concentrations of PVA C_p and glutaraldehyde C_g. In Figure 19, the

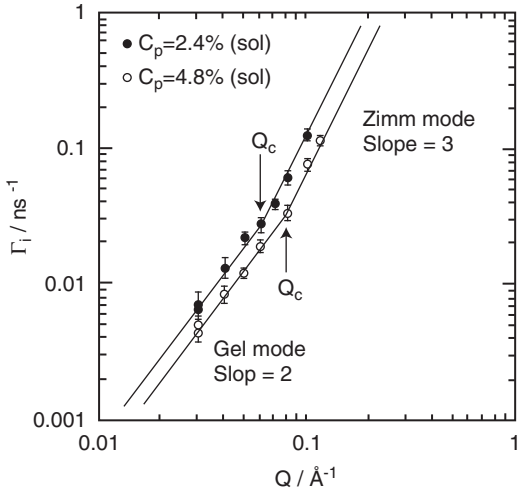

Figure 17 Q dependence of first cumulant Γ_i (initial decay of $\ln[I(Q,t)/I(Q,0)]$) for poly(vinyl alcohol)–borax sol with C_p=2.4 wt% (●) and gel with C_p=4.8 wt% (○).

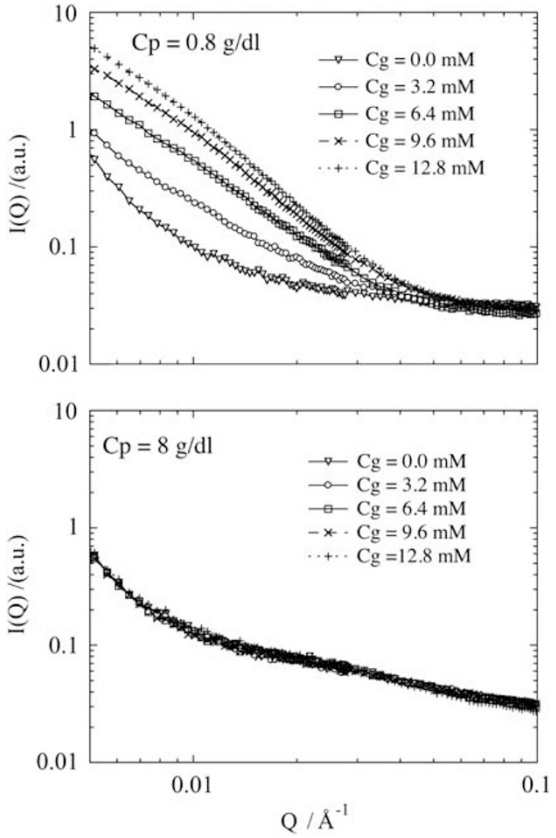

Figure 18 Small-angle scattering intensity $I(Q)$ of chemically crosslinked poly(vinyl alcohol) (PVA) gels for PVA concentrations of C_p=0.8 and 8 g dl^{-1}.

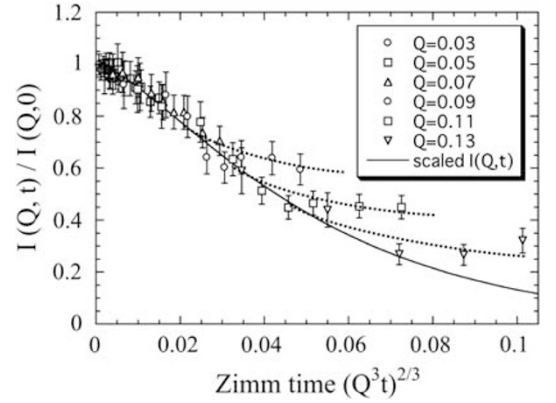

Figure 19 Zimm scaling of normalized intermediate scattering functions $I(Q,t)/I(Q,0)$ of a chemically crosslinked poly(vinyl alcohol) gel for C_p=8 g dl^{-1} and a crosslinker (glutaraldehyde) concentration C_g=6.4 mM. The solid curve is the Zimm master curve; dashed curves are drawn by eye.

observed normalized intermediate scattering function $I(Q,t)/I(Q,0)$ is shown for the gel with C_p=8 g dl^{-1} and C_g=6.4 mM as a function of Q after being scaled by the Zimm time $(Q^3t)^{2/3}$. The Zimm scaling works well in a short time region below about $(Q^3t)^{2/3}$=0.04 ns$^{2/3}$ Å^{-2}, whereas the observed $I(Q,t)/I(Q,0)$ deviated from the Zimm master curve (solid line) and decreased in the long time region (dotted lines), depending on Q. The decrease was clearly caused by the crosslinking in the gel. In the short time region, polymer chains did not undergo the restriction of the crosslinking; they therefore behave as Zimm chain. However, they underwent the restriction of the crosslinking in the long time region, and the motions became slower in the gel than in the solution. Thus, the NSE measurements were able to detect the difference of the dynamic fluctuations, whereas the SANS measurements were not.

SUMMARY

We reviewed our previous studies on the structure and dynamics of PVA gels in mixtures of DMSO and water and in other solvents using various scattering methods. In the structural study, the various scattering methods employed here can cover a very wide Q range from 10^{-4} to 10 Å^{-1}, approximately corresponding to 6 μm to 0.6 Å in real space. In the spatial scale of nanometers to several tens of nanometers, we observed by WANS and SANS measurements that the crosslinking points are crystallites with radii of ∼70 Å and that the distance between the crystallites is 180–200 Å. In addition, the surface of the crystallites is very smooth. The LS studies showed that the SD-type liquid–liquid phase separation at the micrometer scale occurs before gelation at temperatures greater than ∼−20 °C, which results in the polymer-rich and polymer-poor phases. This system exhibits a bicontinuous structure, and crystallization or crosslinking mainly occurs in the polymer-rich phase; the gelation in this phase induces the whole system to form an opaque gel of the bicontinuous structure. However, in the case of transparent homogeneous gels prepared by quenching to a temperature less than ∼−20 °C, spinodal-decomposition-type phase separation of the network occurred against its elasticity involving the volume shrinkage process (syneresis). Finally, we summarized the hierarchic structure of the opaque PVA gel (Figure 12) and the formation mechanism of opaque and transparent gels (Figure 13).

We also studied the dynamics of three kinds of PVA gels: PVA physical gels formed in DMSO/water (60/40), PVA gels formed in aqueous borax solutions and chemically crosslinked PVA gels formed by GA. In the first gel, the static fluctuations were dominant, which shows that the gel is very hard. For the gel in the aqueous borax solution, the NSE measurements showed that polymer chains behaved as if they were in solutions on the spatial scale of several nanometers, which suggests that not all borax molecules participate in the hydrogen bonding to form the crosslinking points. In the third chemically crosslinked gel, the SANS intensities were observed to not depend on the GA concentration (or the crosslinking density) in the gels prepared from a semi-dilute solution (C_p=8 g dl^{-1}), but NSE measurements clearly detected differences in the gels' dynamics.

CONFLICT OF INTEREST

The authors declare no conflict of interest

1 Haehnel, W. & Herrmann, W. O. Vinyl alcohol. *German Patent* 450,286 to Consort.f. elektrochem, Ind. G. m. b. H (1924).
2 Sakurada, I. *Polyvinyl Alcohol Fibers* (Marcel Dekker, Inc., New York, 1985).
3 Herrmann, W. O. & Haehnel, W. *German Patent* 685,048 to Consort.f. elektrochem, Ind. G. m. b. H (1931).
4 Lee, S. Studies on synthetic fiber [Gosei sen-i ni kansuru kenkyu]. *KasenKoenshu* **4,** 51 (1939).
5 Sakurada, I., Lee, S. & Kawakami, H. Manufacturing process of synthetic fiber of poly vinyl alcohol [Pori biniru arukouru kei gousei sen-i no seizouhou]. *Japan Patent* 147, 58 to Nippon Kagaku Sen-iKenkyusho (1939).
6 Lee, S. D., Sakurada, I., Kawakami, H., Hirabayashi, K., Hitomi, K. & Matsuoka, M. Manufacturing process of heat-resistant synthetic fiber of poly vinyl alcohol [Tainetusei takaki pori biniru arukouru kei gousei sen-i no seizouhou]. *Japan Patent* 157, 679 to Nippon Kagaku Sen-iKenkyusho (1940).
7 Pines, E. & Prins, W. Structure-property relations of thermoreversible macromolecular hydrogels. *Macromolecules* **6,** 888–895 (1973).

8 Komatsu, M., Inoue, T. & Miyasaka, K. Light-scattering studies on the sol–gel transition in aqueous solutions of poly(vinyl alcohol). *J. Polym. Sci. Polym. Phys. Ed.* **24,** 303–311 (1986).
9 Hyon, S.- H., Cha, W. & Ikada, Y. Preparation of transparent poly(vinyl alcohol) hydrogel. *Polymer Bull.* **22,** 119–122 (1989).
10 Wu, W., Shibayama, M., Roy, S., Kurokawa, H., Coyne, L. D., Nomura, S. & Stein, R. Physical gels of aqueous poly(vinyl alcohol) solutions: a small-angle neutron-scattering study. *Macromolecules* **23,** 2245–2251 (1990).
11 Shibayama, M., Kurokawa, H., Nomura, S., Muthukumar, M., Stein, R. & Roy, S. Small-angle neutron scattering from poly(vinyl alcohol)-borate gels. *Polymer* **33,** 2883–2890 (1992).
12 Ohkura, M., Kanaya, T. & Kaji, K. Gels of poly(vinyl alcohol) from dimethyl sufloxide/water solutions. *Polymer* **33,** 3689–3690 (1992).
13 Ohkura, M., Kanaya, T. & Kaji, K. Gelation rates of poly(vinyl alcohol) solution. *Polymer* **33,** 5044–5048 (1992).
14 Lee, K. Y. & Mooney, D. J. Hydrogels fot tissue engineering. *Chem. Rev.* **101,** 1869–1879 (2001).
15 Drury, J. L. & Mooney, D. J. Hydrogels for tissue engineering: scafforld design variables and applications. *Biomaterials* **24,** 4337–4351 (2003).
16 Peppas, N. A. & Stauffer, S. R. Reinforcement uncrosslinkedpoly(vinyl alcohol) gels produced by cyclic freezing-thawing processes: a short review. *J. Control. Release* **16,** 305–310 (1991).
17 Takahashi, N., Kanaya, T., Nishida, K. & Kaji, K. Effects of cononsolvency on gelation of poly(vinyl alcohol) in mixed solvents of dimethyl sulfoxide and water. *Polymer* **44,** 4075–4078 (2003).
18 Kanaya, T., Ohkura, M., Kaji, K., Furusaka, M., Misawa, M., Yamaoka, H. & Wignall, G. D. Small angle neutron scattering from poly(vinyl alcohol) gels. *Physica B* **180/181,** 549–551 (1992).
19 Kanaya, T., Ohkura, M., Kaji, K., Furusaka, M. & Misawa, M. Structure of Poly(vinyl alcohol) gels studied by wide- and small-angle neutron scattering. *Macromolecules* **27,** 5609–5615 (1994).
20 Kanaya, T., Ohkura, M., Takeshita, H., Kaji, K., Furusaka, M., Yamaoka, H. & Wignall, G. D. Gelation process of Poly(vinyl alcohol) as studied by small-angle neutron and light scattering. *Macromolecules* **28,** 3168–3174 (1995).
21 Takeshita, H., Kanaya, T., Nishida, K., Kaji, K., Hashimoto, M. & Takahashi, T. Ultra-small-angle neutron scattering studies on phase separation of poly(vinyl alcohol) gels. *Phys. Rev. E* **61,** 2125–2128 (2000).
22 Takeshita, H., Kanaya, T., Nishida, K. & Kaji, K. Small-angle neutron scattering studies on network structure of transparent and opaque PVA gels. *Physica B* **311,** 78–83 (2002).
23 Takahashi, N., Kanaya, T., Nishida, K. & Kaji, K. Small-angle neutron scattering study of poly(vinyl alcohol) gels during melting process. *J. Appl. Polym. Sci.* **95,** 157–160 (2004).
24 Kanaya, T., Takeshita, H., Nishikoji, Y., Ohkura, M., Nishida, K. & Kaji, K. Micro- and mesoscopic structure of poly(vinyl alcohol) gels detemined by neutron and light scattering. *Supramolecular Sci.* **5,** 215–221 (1998).
25 Takeshita, H., Kanaya, T., Nishida, K. & Kaji, K. Gelation process and phase separation of PVA solutions as studied by a light scattering technique. *Macromolecules* **32,** 7815–7819 (1999).
26 Takeshita, H., Kanaya, T., Nishida, K. & Kaji, K. Spinodal decomposition and syneresis of PVA gel. *Macromolecules* **34,** 7894–7898 (2001).
27 Takahashi, N., Kanaya, T., Nishida, K. & Kaji, K. Gelation induced phase separation of poly(vinyl alcohol) in mixed solvents of dimethyl sulfoxide and water. *Macromolecules* **40,** 8750–8755 (2007).
28 Kanaya, T., Takahashi, N., Nishida, K., Kaji, K., Seto, H., Nagao, M., Kawabata, Y. & Takeda, T. Neutron spin echo studies on poly(vinyl alcohol) gel in a mizture of dimethyl sulfoxide and water. *J. Neutron Res.* **10,** 149–153 (2002).
29 Kanaya, T., Takahashi, N., Nishida, K., Seto, H., Nagao, M. & Takeda, T. Neutron spin-echo studies on dynamic and static fluctuations in two types of poly(vinyl alcohol) gels. *Phys. Rev. E* **71,** 011801-1–011801-7 (2005).
30 Kanaya, T., Takahashi, N., Nishida, K., Seto, H., Nagao, M. & Takeda, Y. Dynamic and static fluctuations in polymer gels studied by neutron spin-echo. *Physica B* **385–386,** 676–681 (2006).
31 Ishikawa, Y., Furusaka, M., Niimura, N., Arai, M. & Hasegawa, K. SAN at KENSThe time-of-flight small-angle scattering spectrometer SAN at the KENS pulsed cold neutron source. *J. Appl. Cryst.* **19,** 229–242 (1986).
32 Ito, Y., Imai, M. & Takahashi, S. Small-angle neutron scattering instrument of the institute for solid state physics, University of Tokyo (SANS-U). *Physica B* **213/214,** 889–891 (1995).
33 Koehler, W. C. The national facility for small-angle neutron scattering. *Physica B* **137,** 320–329 (1986).
34 Takahashi, T. Ultra small angle scattering instrument (ULS). *Activity Report on Neutron Scattering Research*, Neutron Scattering Laboratory, Institute for Solid State Physics, University of Tokyo, Tokyo, Japan. **1,** 34–35 (1994).
35 Oberthuer, R. C. Radius of gyration versus molar mass relations from light scattering for polydisperse non-gaussian chain molecules. polystyrene in toluene and short DNA-fragments in aqueous NaC1-solution. *Makromol. Chem.* **179,** 2693–2706 (1978).
36 Shibatani, K. Gel formation and structure of junctions in poly(vinyl alcohol)–water systems. *Polym. J.* **1,** 348–355 (1970).
37 Takahashi, A. & Hiramitsu, S. The melting temperature of a thermally reversible gel. III. poly(vinyl alcohol)—water gels. *Polym. J.* **6,** 103–107 (1974).
38 Flory, P. J. Theory of crystallization in copolymers. *Trans. Faraday Soc.* **51,** 848–857 (1955).
39 Guinier, A. & Fournet, G. *Small-Angle Scattering of X-rays*, John Wiley, New York, 1955.
40 Flory, P. J. *Principles of Polymer Chemistry*, Cornell University Press, Ithaca, NY, 1957.
41 Kaji, K., Urakawa, H., Kanaya, T. & Kitamaru, R. Distance distribution analysis of small-angle X-ray scattering for semidilute polyelectrolyte solutions without salts. *Macromolecules* **17,** 1835–1839 (1984).
42 Cahn, J. W. Phase separation by spinodal decomposition in isotropic systems. *J. Chem. Phys.* **42,** 93–99 (1965).
43 Cahn, J. W. & Hilliard, J. E. Free energy of a nonuniform system. I. interfacial free energy. *J. Chem. Phys.* **28,** 258–267 (1958).
44 Mezei, F. *Neutron Spin Echo* Vol. 128Springer Verlag, Berlin, 1980.
45 Springer, T. *Quasielastic Neutron Scattering for the Investigation of Diffusive Motions in Solids and Liquids* Vol. 64.Springer, Verlag, Berlin, 1972.
46 Takada, A. & Nemoto, N. Dynamics of associating polymers in solution: dynamic light scattering and dynamic viscoelasticity of poly(vinyl alcohol) in aqueous borax solution. *Progr. Colloid Polym. Sci.* **106,** 183–187 (1997).
47 Takada, A., Nishimura, M., Koike, A. & Nemoto, N. Dynamic light scattering and dynamic viscoelasticity of poly(vinyl alcohol) in aqueous borax solutions. 4. further investigation on polymer concentration and molecular weight dependencie. *Macromolecules* **31,** 436–443 (1998).
48 Zimm, B. H. Dynamics of polymer molecules in dilute solution: viscoelasticity, flow birefringence and dielectric loss. *J. Chem. Phys.* **24,** 269–278 (1956).
49 Ewen, B. & Richter, D. Neutron spin echo investigation on the segmental dynamics o polymers in melts, networks and solutions. *Adv. Polym. Sci.* **134,** 1–129 (1997).
50 Dubois-Violette, E. & de Gennes, P. G. Quasi-elastic scattering by dilute, ideal, polymer solutions: II. Effects of hydrodynamic interactions. *Physics* **3,** 181–198 (1967).
51 Tanaka, T., Hocker, L. O. & Benedek, G. B. Spectrum of light scattered from a viscoelastic gel. *J. Chem. Phys.* **59,** 5151–5159 (1973).